

REVISION 1

D-poor Hydrogen in Lunar Mare Basalts Assimilated from Lunar Regolith

Allan H. Treiman^{1*}, Jeremy W. Boyce^{2,3}, James P. Greenwood⁴, John M. Eiler², Juliane Gross⁵, Yunbin Guan²,
Chi Ma², Edward M. Stolper²

¹ Lunar and Planetary Institute, 3600 Bay Area Boulevard, Houston, TX 77058

² Division of Geological & Planetary Sciences, Caltech, 1200 E. California Blvd., Pasadena, CA 91125

³ Department of Earth, Planetary, and Space Sciences, UCLA

⁴ Department of Earth & Environmental Sciences, Wesleyan University, Middletown, CT 06459

⁵ Department of Earth and Planetary Sciences, Rutgers University, 610 Taylor Rd., Piscataway NJ 08854

*Correspondence to: Allan H. Treiman (treiman@lpi.usra.edu).

Abstract

Apatite grains in lunar mare basalts contain hydrogen that ranges in D/H ratio by more than a factor of two. For most of these basalts, the D/H ratios in their apatite grains decrease with measures of the host basalts' time spent at elevated temperature, specifically the Fe-Mg homogenization of their pyroxenes. Most basalts with homogeneous pyroxenes (i.e., with constant Fe/Mg ratio) have apatite grains with low D/H ($\delta D \approx -100\text{‰}$), whereas most basalts with heterogeneous pyroxenes (i.e., varying or zoned Fe/Mg) have apatite with high D/H (δD up to $\sim +1100\text{‰}$). This relationship suggests that low D/H values were acquired during thermal processing, i.e. during Fe-Mg chemical equilibration, during or after emplacement. This light hydrogen is likely derived from solar wind implanted into the lunar regolith (with δD from -125‰ to -800‰), and could enter basalts either by assimilation of regolith or by vapor transport from regolith heated by the flow. If a basalt could not interact with regolith rich in solar wind (e.g., it was emplaced onto other fresh basalts), its apatite could retain a magmatic D/H signature. The high D/H component (in the apatites of unequilibrated basalts) is most reasonably that indigenous magmatic hydrogen, i.e. representing hydrogen in the basalt's source mantles, or magmatic hydrogen that was residual after partial degassing of H_2 .

Keywords: mare basalt, hydrogen isotopes, lunar regolith.

Introduction

The inferred abundances of volatile species in the Moon have changed drastically over the last decade – from nearly absent, to as abundant as in the Earth (Saal et al., 2008; Boyce et al., 2010; McCubbin et al., 2010; Elkins-Tanton and Grove, 2011; Greenwood et al., 2011; Hauri et al., 2011; Hui et al., 2013; McCubbin et al., 2015). The inferred abundance of hydrogen is central to this change of view, and hydrogen bears special importance in petrology, astrobiology, and resources for human habitation. Hydrogen has two stable isotopes, hydrogen proper and deuterium, and their abundance ratio D/H is a crucial clue to the histories of volatiles in the Moon, and its samples.

The D/H ratio is particularly useful for the Moon because its materials span a huge range in D/H, from essentially zero to six times that of standard seawater – in the common δD notation¹ from -900‰ to ~+5000‰, (Liu et al., 2012a; Saal et al., 2013; Tartèse et al., 2014a). Lunar δD values have been measured in many types of materials, including: the mineral apatite, see Figure 1 (Greenwood et al., 2011; Barnes et al., 2013; Tartèse et al., 2014a); igneous glasses and melt inclusions (Saal et al., 2008; Saal et al., 2013; Chen et al., 2015; Hauri et al., 2015); regolith and its agglutinates (Epstein and Taylor, 1973; Liu et al., 2012a); and the minerals plagioclase (Hui et al., 2015), pyroxene, and olivine (Liu et al., 2012b). Some of the highest δD values reflect production of D by cosmogenic spallogeneis (Saal et al., 2013; Tartèse et al., 2014a), which is most significant for hydrogen-poor materials (Stephant and Robert, 2014; Treiman et al., 2014). After corrections for spallogenic D, lunar δD values still range up to ~+4200‰ (Saal et al., 2013).

¹ The ‘ δ ’ notation gives the deviation, in parts per thousand, of the abundance ratio of the uncommon to the common isotope, relative to the abundance ratio of a standard, e.g., $\delta D = \left[\frac{(D/H)_{unk} - (D/H)_{std}}{(D/H)_{std}} \right] \times 1000$, where the standard is VSMOW.

The mineral apatite, $\text{Ca}_5(\text{PO}_4)_3(\text{F},\text{Cl},\text{OH})$, is central to understanding lunar H and other volatiles, because it is widespread (although of low abundance) in lunar rocks and regolith, and is the only currently known crystalline phase on the Moon that requires volatile species. The volatile element compositions of apatite have been used widely as a monitor of volatile element (H, C, F, S, and Cl) abundances and behaviors in geological systems, both planetary (Watson et al., 1994; Boctor et al., 2003; Boyce et al., 2010; McCubbin et al., 2010; Greenwood et al., 2011) and terrestrial (O'Reilly and Griffin, 2000; Patiño Douce and Roden, 2006; Boyce and Hervig, 2008; Boyce and Hervig, 2009).

Interpretations of this large range in lunar δD in lunar apatite (after correction for spallogenesis) are many and varied, both in terms of processes and components. Components that may contribute to lunar H signatures include: primordial material from Moon formation; residual silicate melt from the lunar magma ocean, i.e. the KREEP component (Tartèse et al., 2014b), cometary infall (Greenwood et al., 2011), meteoritic infall (Tartèse and Anand, 2013; Füre et al., 2014), and solar wind implanted in the regolith or crust (Liu et al., 2012a). Processes that could have modified or redistributed hydrogen from these components include: magma degassing (Anand et al., 2014; Füre et al.; Tartèse et al., 2014a), igneous crystallization-fractionation (Boyce et al., 2014), condensation and adsorption onto regolith (Pieters et al., 2009; Dyar et al., 2010), and exchange during metamorphism/metasomatism (Taylor et al., 2004; Treiman et al., 2014).

Collectively, hydrogen in apatites from all mare basalts falls into two group, as shown in Figure 1. Among high-Ti and low-Ti basalts, there is a rough trend of increasing δD with decreasing H_2O content, Figure 1 and Fig. 3 of Tartèse et al. (2013). Tartèse et al. (2013) interpreted the wide range of δD values in the mare basalt apatites as arising by degassing of large proportions (varying by basalt sample) of H_2 from the basalts before and during apatite crystallization. There is also a cluster of analyses at low H and low δD , most of which represent KREEP-rich basalts (Tartèse et al., 2014b), notably 72257 and NWA 773, see Figure 1B of Tartèse et al. (2014b).

Here, we show that the δD values of apatites in lunar mare basalts decrease with increasing measures of the time the basalts spent at high temperature – specifically the Fe-Mg homogeneities of their pyroxenes – independent of basalt type. This relationship suggests that δD values were modified during that thermal history, and thus that the trends of H abundance and δD reflect mixing rather than degassing. We present a model of this process, in which the apatites (and their host basalts) contained D-rich hydrogen ($\delta D > +900\text{‰}$) during or just after eruption, which was mixed with and replaced by D-poor hydrogen ($\delta D \leq \sim -100\text{‰}$) during their thermal processing. This D-poor hydrogen component, which is constrained by the lowest δD analyzed in apatites of lunar mare basalts, can reasonably be ascribed to the lunar regolith, and would represent a mixture of contributions from solar wind, outgassing, and exogenous solid infall.

Samples

Six thin sections of five mare basalt samples were analyzed by ion microprobe for this study: two high-Ti basalts (10044,12, and ,644; 75055,55); and three low-Ti basalts (12039,42; 12040,211; MIL 05035,6). All these mare basalts contain small grains of apatite ($>100 \mu\text{m}$) in their mesostases, consistent with late crystallization of apatite from their magmas. Mare basaltic rocks experienced a wide range of thermal histories, from quenched glasses associated with fire fountains to ‘micro-gabbros,’ in which Fe and Mg have completely equilibrated across and among pyroxenes and olivines. Figure 2 shows two examples of apatite grains in mare basalts, one with chemically zoned pyroxene grains, and the other with fully equilibrated pyroxenes. See the Online Deposit Material for additional information on the samples analyzed here, including petrography and images of their apatite grains. Data on other samples are from the literature, to which the reader is referred (Table S2). However, two literature samples require explanation.

The lunar meteorite NWA 773 and its pairs are breccias of basaltic materials (Zeigler et al., 2007) with abundant large clasts of olivine gabbro (Fagan et al., 2003; Jolliff et al., 2003). Here, we use only analyses from

the olivine gabbro lithology, both of its apatite (ROI13 of (Tartèse et al., 2014a)) and its ferromagnesian minerals (Fagan et al., 2003). NWA 773 has a cosmic ray exposure age of ~155 My (Fernandes et al., 2003; Lorenzetti et al., 2005).

The lunar meteorite NWA 4472 and its pair NWA 4485 are breccias (a “smørgasbord”, (Joy et al., 2011)) of basaltic and KREEP-rich fragments with rare fragments of highlands material. Joy et al. (2011) described a unique apatite-rich fragment, 500 μm by 500 μm , with ilmenite and ferroan pyroxene; they analyzed its apatite rare earth elements and U-Pb isotopes, and Tartèse et al. (2014a) analyzed its apatite for H and Cl abundances and isotopes. This clast is not representative of a larger rock body (being so rich in apatite and lacking plagioclase and olivine), and Joy et al. (2011) infer that it represents a late fractionate from a KREEP-rich basalt. We infer further that the apatite-rich fragment is related to the other KREEP-rich basalt in NWA 4472, the lithology 8 of Table 1 in Joy et al. (2011). So, we used the analyses of apatite in that clast (Tartèse et al. (2014a) in concert with the compositions of ferromagnesian minerals of the meteorite’s KREEP basalt (Joy et al., 2011). The cosmic ray exposure age of NWA 4472 has not been reported.

Our analyses of apatite in these samples are compared with data from the published peer-reviewed data hydrogen abundances and isotope ratios in other lunar mare basalts. Relevant analyses in gray literature (e.g., abstracts of conference presentations) are discussed individually as needed.

Methods

Analyses for H, D/H, and Cl in these mare basalt apatites were obtained at the Caltech Center for Microanalysis using a Cameca 7f-GEO secondary ion mass spectrometer following standard protocols (Treiman et al., 2014). Data on H and D/H are given in Table 1; data for Cl and F on these same apatite grains are reported in Boyce et al. (2015) and Table S1. Standards used for abundance measurements are those of McCubbin et al. (2010), with the slightly revised values of Boyce et al. (2012). Isotopic measurements are reported relative to Durango apatite, which has $\delta\text{D} = -120 \pm 5\%$ (Greenwood et al., 2011). Abundances of H

come from measuring $^{16}\text{O}^1\text{H}$, ^{18}O (the reference element), and ^{31}P (a secondary reference element) using a 0.5 nA, $\sim 15\text{keV}$ Cs^+ beam at a mass resolving power of ~ 5500 m/ Δ m. These analyses also included measurements of abundances of ^{35}Cl and $^{37}\text{Cl}/^{35}\text{Cl}$, which are reported in Boyce et al. (2015) and the Online Deposit Materials. The 2σ detection limit for H_2O in apatite is ~ 20 ppm. Measurements of H isotope ratios were made on H^+ and D^+ ions, detected by electron multiplier, over 50-100 cycles of rastering at $\sim 3\text{nA}$ across a $2\mu\text{m} \times 2\mu\text{m}$ area, preceded by 180 sec of presputtering by a $\sim 3\text{nA}$ beam rastered across a $25\mu\text{m} \times 25\mu\text{m}$ area. See Deposit Material for more analytical details, the calibration curve for H_2O (Figure S8), and all analytical results (Tables S1 and S2).

We calculated the proportion of D that would be contributed by spallogenesis to the hydrogen in the apatite following Reedy (1981). For apatite in 10044 and 75055, both with cosmic ray exposure (CRE) ages of ~ 80 my (Meyer, 2012), the spallogenic contribution of D is insignificant. For 12039, we can find no published CRE age; however, its apatites contain enough H that the spallogenic D contribution is likely to be insignificant. Only for apatite in 12040, which has a long exposure age of 285 ± 50 m.y. (Burnett et al., 1975) and little H, is spallogenic D significant; its corrected δD values are distinctly lower than the measured values (Table 1, Table S1). We have not corrected for spallogenic production of H (Merlivat et al., 1976), because the reported production rate has not been confirmed. Were that correction included, only the δD values for 12040 in Table 1 would be affected, and then only by small proportions that would not be noticeable in the Figures.

Our new analyses are consistent with, and complement literature analyses of apatites from other sections of the same mare basalts, as discussed below.

Results

Hydrogen abundances and hydrogen/deuterium ratios in apatites in mare basalts vary widely, as has been reported elsewhere, e.g. Tartèse et al. (2013). Hydrogen abundances in our analyses (blank-corrected) range

from 3 to 3000 ppm wt. H₂O equivalent, with 2 σ detection limit of 20 ppm (Table S1, in Deposit Materials). This range is lower than the highest reported H₂O equivalent in a mare basalt apatite, ~16500 ppm (Tartèse et al., 2014a). In our analyses, apatite grains in low-Ti mare basalts have H concentrations ranging from < 100 ppm H₂O equivalent (12040) to 2920±60 2 σ^2 ppm H₂O equivalent (12039; Fig. 3). Apatites from high-Ti mare basalts (10044 and 75055) contain between 420±20 and 1430±30 ppm H₂O equivalent. Apatite in many basalt samples shows intra- and inter-grain variability in H abundance beyond analytical uncertainties (Table S1, in Deposit Material)

In our analyses, δ D of mare basalt apatites also varies widely, with typical ranges across a single sample of ~400 ‰. Apatite grains in low-Ti basalt 12039 have a small range in δ D, only from +700±30‰ to 830±30‰ (N=4). Other samples are more variable: apatites from (high-Ti basalt) 75055 range from δ D of +620±40‰ to +970±30‰ (N=4), apatites in 10044 range from δ D of +540±60‰ to +950±30‰ (N=6), Figure 3. The ranges we observed for 10044 are consistent with other analyses of that basalt (Greenwood et al., 2011; Barnes et al., 2013). As with H abundances, intra- and inter-grain variability in δ D are larger than analytical uncertainties (Greenwood et al., 2011; Pernet-Fisher et al., 2014; Tartèse et al., 2014a), and must represent real heterogeneities.

12040

The apatites in 12040 contain the least H of those analyzed here, Table 1 and see Greenwood et al. (2011), and the rock had a long exposure to cosmic rays on the lunar surface. We obtained H and δ D analyses of individual target spots on three apatite grains from the same thin section as did Greenwood et al. (2011), see

² All uncertainties are 2 σ (standard deviation) of counting or population (whichever is larger), unless otherwise noted.

Table 1 and Table S1. Two of our analyses show water abundances of 3 and 16 ppm H₂O, which are below our detection limit (~20 ppm). The other analysis (point 1, Table 1) averages 105 ppm H₂O (blank-subtracted), which is a detection at 10 σ of counting statistics. We interpret this analysis as representing indigenous H in the apatite of 12040, as the abundance seems too high to represent only adsorbed water.

The apatite analysis in 12040 with the highest H₂O abundance, point 1, has a nominal $\delta D = +9 \pm 165\%$ (Table 1), which is consistent with earlier data (Greenwood et al., 2011). That value must be corrected for spallogenic D and H because of the rock's long exposure age, 285 ± 50 m.y. (Burnett et al., 1975). Spallogenesis of deuterium in lunar samples is calculated (and experimentally confirmed) to be 0.92×10^{-12} mole D / gm-My (Merlivat et al., 1976; Reedy, 1981). Correcting for spallogenic D at the nominal exposure age gives a pre-spallogenic $\delta D = -20\%$. However, the exposure age is uncertain (as above) and the D production rate must be considered uncertain. So, we calculated D abundances and δD values for the range of exposure ages and for spallogenic production rates at twice and half those of Merlivat et al. (1976) and Reedy (1981). With these ranges of ages and rates, the calculated pre-spallation δD of 12040 point 1 is between -3% and -59% (Table S1). Combining the uncertainties of counting statistics, calibration, and spallogenesis corrections gives a total uncertainty on the analysis of near $\pm 200\%$, which is shown in Table 1 and Figure 3.

Discussion

In our results, there are two main issues to explain: the variability in the compositions of apatites in a sample, and the process(es) responsible for the differences in δD among samples.

Intra-sample Elemental and D/H Variability

Two explanations have been offered to explain systematic variations in abundances of H, Cl, and F in lunar mare apatites. The first is degassing, in which low-H apatites have been interpreted as having crystallized from late melts that were depleted in H and Cl compared to F (Tartèse and Anand, 2013). The second is igneous

fractionation, in which high-H apatites crystallized from late melts that had already fractionated F-rich apatite (Boyce et al., 2014). Although both processes are likely to occur in mare basalts, large apatite phenocrysts with core to rim variations in H, Cl, and F can be used to test which of the two mechanisms for generating variations is dominant. Such apatite crystals are present in basalts 12039 (Greenwood et al., 2011), 10044 (Greenwood et al., 2011), and 14053 (McCubbin et al., 2010); in all three cases, the core of apatite crystals are enriched in F relative to H and Cl, whereas H and Cl are enriched over F in the rims, with H/Cl increasing from core to rim (Boyce et al., 2014). Assuming that the apatite cores grew first, and that the rims (and terminations) grew later, these compositional trends indicate that magmatic fractionation of apatite is likely responsible for the majority of variations in H and Cl abundances in lunar mare apatite (Boyce et al., 2014).

Apatite grains in mare basalts also show significant intra-sample variability – different grains in a rock can have distinct δD values (i.e., D/H ratios). These intra-sample ranges are typically outside analytical uncertainties (Table 1), and can be up to several hundreds per mil in δD (Greenwood et al., 2011; Barnes et al., 2013; Tartèse et al., 2014a). Such large variability in δD is seen even in samples with evidence of extended thermal histories, like the olivine cumulate lithology of NWA 773 (Table S2, Tartèse et al. (2014b)).

D/H Variation Among Samples

Lunar mare apatites show a wide range of δD values (Greenwood et al., 2011; Barnes et al., 2013; Tartèse and Anand, 2013) with δD ranging from -277‰ to ~+1200‰ (Anand et al., 2014). The range of analyzed δD includes intergrain and intragrain variability among apatites in an individual basalt sample (Figure 1, see Table S2 for data and sources), and variations among samples and to a lesser extent between different analysts' averages for a given sample (Table S2).

The cause of this intra-sample variability in δD is not known with certainty. Greenwood et al. (2011) ascribed this range in δD as variable mixing of solar wind H implanted into the rocks (low δD) with a cometary

hydrogen component (high δD), both mixed with a primordial H component similar to that in the Earth's mantle. The heavy hydrogen of cometary origin could have come from assimilation of regolith rich in cometary debris, or from cometary material mixed into the lunar mantle in the distant past. From their data, they conclude that “[T]he lack of correlation between H_2O and δD of individual lunar apatite grains ... would seem to rule out an origin for elevated δD of lunar water by the processes of degassing of water or hydrogen, subsolidus diffusion of hydrogen, or dehydration reactions...”, see Figure 1 here (and Figure S9 in Deposit Materials).

Summarized data on apatites from non-KREEPy basalts (Tartèse and Anand, 2013) shows a larger range of δD values and H_2O abundances, which are roughly anti-correlated with each other, Figure 1 here and Fig. 3 of Tartèse et al. (2013). This relationship is consistent, in broad brush, with variable degrees of H_2 degassing from basaltic magmas, with different degrees of degassing for each magma, see Fig. 2 of Tartèse and Anand (2013) and Fig. 8b of Tartèse et al. (2013) for the high-Ti mare basalts. This degassing would have happened before and during crystallization of apatite; thus its timing and extent in a particular sample depend on: the original vapor content of the parent magma; the original phosphorus content of the magma (which controls the temperature of apatite crystallization), and the pressure at which the magma crystallized. (Tartèse et al., 2013; Tartèse et al., 2014a; Tartèse et al., 2014b). Lunar basaltic glasses show a similar trend of increasing δD with decreasing H_2O , which has been interpreted as a result of degassing (Füri et al., 2014).

D/H Correlates with Thermal History

As partial explanation of the range of hydrogen isotope values in mare basalt apatites, we find that their δD is correlated with measures of their basalts' thermal histories, specifically the extents of Fe-Mg chemical zoning of their pyroxenes. In a rapidly cooled basalt, pyroxene would be strongly zoned, with early material being magnesian and later being ferroan. In a basalt that cooled slowly, this Fe-Mg zoning would diffuse toward homogeneity (Cherniak and Dimanov, 2010). A qualitative measure of the integrated thermal history of the sample is $Mg\#_{min}/Mg\#_{max}$ in its mafic silicate minerals, where $Mg\#$ is the molar ratio $Mg/(Mg+Fe)$, and 'min'

and ‘max’ refer to the minimum and maximum values reported (Meyer, 2012). This index is a qualitative or ordinal measure of thermal history because it cannot account for important variables like: initial Mg# of the magma, the Ti content of the magma (high-Ti mare basalts contain more magnesian pyroxenes, as their Fe is sequestered in ilmenite), highest Mg# of the pyroxene (which depends on the crystallization sequence), and changes in Fe-Mg diffusion with temperature, and the number of analyses reported for the sample.

Apatites in basalts with chemically homogeneous pyroxenes (low $Mg\#_{max}/Mg\#_{min}$) have uniformly low δD values of approximately -100‰, Figure 3. On the other hand, apatites in basalts with extensive Fe-Mg zoning in their pyroxenes (high $Mg\#_{max}/Mg\#_{min}$) have high δD (Figure 3). From Figure 3, one could argue for a regular monotonic relationship between apatite δD and $Mg\#_{max}/Mg\#_{min} - \delta D$ declines as Fe-Mg homogenization proceeds, except for sample 14053 which has a unique history (Taylor et al., 2004). However, a simple monotonic relationship may not be real or reasonable, because: [1] $Mg\#_{max}/Mg\#_{min}$ does not necessarily measure the appropriate thermal timescales related to hydrogen mobility; [2] $Mg\#_{max}/Mg\#_{min}$ is not a linear measure of thermal history, because most of the range of Mg# in a typical igneous pyroxene grain is seen in a thin zone at its edge (e.g., Treiman (2005)); and [3] $Mg\#_{max}/Mg\#_{min}$ values taken from the literature are of variable and unknown qualities (Meyer, 2012). Even with these caveats, it is clear that most extensively equilibrated basalts (low $Mg\#_{max}/Mg\#_{min}$) have distinctly lower δD than do unequilibrated mare basalts.

It is also clear from Figure 3 that the general correlation between δD and Fe-Mg equilibration is independent of basalt type. Most of the available data are for low-Ti mare basalts, and they span nearly the full range of δD and pyroxene $Mg\#_{max}/Mg\#_{min}$ (the unusual result for 12018 is discussed below). The few samples of high-Ti and KREEP basalts are consistent with the $\delta D - Mg\#_{max}/Mg\#_{min}$ trend of the low-Ti basalts, as is the single VLT sample. The single analyzed high-Al basalt sample (14053) falls off of the trend, but it has a unique post-eruptive metasomatic history and may not be representative of high-Al basalts as a group (Taylor et al., 2004).

It is also noteworthy that the abundance of H₂O in mare basalt apatites not correlated with the range of Mg# in their pyroxenes, see Figure 4. The mare basalts with the most H₂O-rich apatite grains include some of the most- and least-equilibrated; similarly, the mare basalts with the H₂O-poorest apatites include both highly- and minimally-equilibrated samples. Comparison of Figures 3 and 4 shows (as does Fig. 1) that the δD of a mare basalt apatite is not correlated with its H₂O content.

The source of the low δD hydrogen in apatites of equilibrated basalts must have δD less than approximately -100‰, the lowest value measured in the apatites of equilibrated lunar basalts. Lunar regolith is the most obvious available source of H encountered by erupted and shallowly emplaced lunar magmas; its average δD is not known well, although the few available bulk analyses give δD values in the range of -400‰ to -800‰ (Friedman et al., 1970; Epstein and Taylor, 1973). Analyses of individual agglutinate particles in lunar regolith show a huge range of δD values, from -800‰ to +4200‰ (Liu et al., 2012a); the latter high value is interpreted to represent a meteoritic hydrogen component. Epstein and Taylor (1973) found that oxygenated hydrogen (H₂O as opposed to H₂) in several regolith samples approached $\delta D \approx -125$ ‰, but ascribed that value to pervasive terrestrial contamination. However, Friedman et al. (1974) interpreted the similar δD of rusty rock 66095 (-75‰ to -175‰; see Robinson and Taylor (2014)) as representing indigenous lunar hydrogen. Similarly, hydrogen in apatite in 14053, which is interpreted as deriving in part from solar wind (Taylor et al., 2004) has δD of ~ -200 ‰, see Table 1 (Greenwood et al., 2011). Hydrogen in the lunar regolith is a large-scale, long-term mixture of many possible components, including indigenous sources (e.g., basalt outgassing), solar wind, meteoritic infall and cometary infall (Liu et al., 2012a), all modified by diurnal mobility (Pieters et al., 2009) and subsequent fractionations (Liu et al., 2012a). The observation that the H₂O contents of apatites from equilibrated basalts are not correlated with their δD (Figs. 3 & 4) suggests that the former was not set during the metamorphic/metasomatic event that set the latter. Thus, it seems reasonable to infer that the low δD of the

apatites in equilibrated basalts arose by diffusion and exchange of H and D into the apatites, and not by diffusion of OH and OD in exchange for F and Cl in the apatite.

It is not clear that the minimum δD we analyzed reflects complete D-H equilibration with a regolith source; e.g., oxidized H as suggested by Friedman et al. (1974) or reflects partial equilibration with a regolith source of lower δD (Epstein and Taylor, 1973; Liu et al., 2012a). However, Barnes et al. (2014), Anand et al. (2014), and Furi et al. (2014) interpret hydrogen with similar δD as representing an indigenous lunar component.

Hydrogen isotope fractionation during magmatic degassing (Saal et al., 2013; Tartèse and Anand, 2013) should not produce the observed correlation of δD and mineral homogeneity (Figure 3), but should have produced the opposite – with more time to degas, the equilibrated basalts should show greater δD . On the other hand, H_2 degassing during equilibration should yield apatites in the equilibrated basalts with less hydrogen (and chlorine) and more fluorine, which is observed at least for H (Fig 4).

The physical mechanism for introduction of regolith H into the apatite of mare basalts is likely to be thermal degassing of the regolith, induced by the heat of the basalts themselves or of nearby impact events (Fagents et al., 2010; Rumpf et al., 2013; Stephant and Robert, 2014; McCubbin et al., 2015). Metasomatism like this has been demonstrated for a few lunar samples (Taylor et al., 2004; Treiman et al., 2014), and we suggest that it may be a common process in modifying the hydrogen isotope compositions in lunar materials. Another feature of this mechanism is that it can explain the large range in δD observed among individual samples and among grains in a single sample; the variation would naturally arise during channelized intergranular transport of D-poor hydrogen-bearing vapor and exchange between that vapor and apatites. We did not note significant petrographic differences among apatite grains with differing δD .

The high δD hydrogen in apatites in basalts with limited Fe-Mg exchange represents a component that was inherent to the basalt as apatite crystallized, though not necessarily to the magma as emplaced nor its

mantle source(s). That component must have had δD at or above the highest values reported here, i.e., $\geq \sim +800\text{‰}$, and could have arisen in several ways: as an indigenous mantle component (Greenwood et al., 2011); a product of H_2 loss during a magma ocean phase from an original δD similar to that of the Earth; or by degassing of H_2 by low- δD magmas on emplacement and before apatite saturation (Barnes et al., 2013; Saal et al., 2013; Tartèse et al., 2013; Hauri et al., 2015; Ustunisik et al., 2015). If the last is generally correct, that the high- δD values of apatite in minimally equilibrated basalts (Fig. 3) represent degassing on emplacement, then no basalt analyzed here or reported in the literature retains a significant proportion of its original low- δD hydrogen. Such a hypothetical basalt, with original low- δD hydrogen and not degassed, would also not have had time for Fe-Mg equilibration in its minerals, and should plot on Figure 3 at low- δD and low Mg_{\min}/Mg_{\max} . Only 14053 plots in that vicinity in Figure 3, but the low- δD hydrogen in its apatite is demonstrably from interaction with solar wind hydrogen (Taylor et al., 2004).

Exceptions That ‘Prove the Rule’

Some mare basalts do not follow the above hypothesis (Figure 3), and provide “real world” evidence on the limitations of the hypothesis and the complications of the lunar environment.

Basalt 14053 is such an exception, with unequilibrated pyroxenes and apatite with low δD , Figure 3 (Taylor et al., 2004; Boyce et al., 2010). Its unique history, rapid crystallization followed by an intense (but short) heating event in the presence of solar-wind hydrogen (Taylor et al., 2004), shows both the potential rapidity of hydrogen exchange between apatite and implanted solar wind, and the potential importance of impact processes in hydrogen metasomatism. Based on this model, one could imagine a basaltic impact melt developed from basaltic regolith rich in solar-wind hydrogen. That impact melt might crystallize to develop extensively zoned pyroxenes (Fagan et al., 2013) and retain the low δD of its source regolith.

Basalt 12018 is exceptional in the opposite way – extensively equilibrated pyroxenes but very high δD in its apatite grains, Figure 3 (Greenwood et al., 2014) – that highlights the potential importance of local environment. A basalt cannot be affected by hydrogen metasomatism if no hydrogen is available, no matter how long the basalt stays hot. So, a basalt flow emplaced onto fresh basalt or very young regolith will have no accessible source of solar-wind hydrogen, and will retain the δD it had on emplacement (or on degassing). So, one should expect some proportion of slowly cooled basalts to have high δD values. On the other hand, there is no guarantee that hydrogen in the lunar regolith necessarily is dominated by a solar wind contribution. For example, the volatile enrichment in lunar soil 61221 may reflect cometary material (Gibson and Moore, 1973), regolith agglutinate grains have a wide range of δD values (Liu et al., 2012a), and comets (and micrometeorites) span a wide range of D/H ratios (Greenwood et al., 2011; Hartogh et al., 2011; Alexander et al., 2012; Altwegg et al., 2015).

Implications

Our results show that the hydrogen isotopic compositions of most mare basalts represent mixing of a heavy component, $\delta D > \sim +800\text{‰}$ and a light component, $\delta D \leq \sim -100\text{‰}$. The light component is inferred to represent hydrogen in lunar regolith, which entered the basalts during their thermal histories (igneous and post-igneous) – the longer and higher temperature a basalt experienced, the more regolith-like its D/H can become. Our data do not constrain the origin of the high- δD component; it could represent H remaining in the basalts after extensive fractionating degassing of a magmatic low- δD component (Saal et al., 2008; Barnes et al., 2013; Tartèse et al., 2013; Hauri et al., 2015; Ustunisik et al., 2015). However, we see no direct evidence of such a low- δD magmatic component.

Acknowledgments: All data generated for this study are available in the online Deposit Material. The second author acknowledges support received from coauthors and colleagues during this project, which was considerably lengthened by a near-fatal illness. We are grateful to: the institutions and people who made samples available for his research, including the Lunar Sample and Meteorite curators at Johnson Space Center; F. McCubbin and J. Mosenfelder, who provided apatite and other mineral standard materials; K. Joy for valuable discussions. The manuscript was improved substantially by reviews, especially that by R. Tartése, to whom we are particularly grateful; we also thank five anonymous reviewers. This research was supported by NASA Early Career Fellowships to Boyce (NNX13AG40G), as well as NASA grants to Treiman and Gross (NNX12AH64G) and Greenwood (NNX11AB29G). The authors have no competing interests. LPI Contribution #1xxx.

Tables

Table 1. Analyses of H in apatites in mare basalts.

sample	section	point	H ₂ O (ppm)*	H ₂ O (ppm) 2σ	δD* ‰	δD corr. ‡ ‰	δD 2σ ‰	Basalt Type
10044	12	10	1105	29	933	932	31	High Ti
10044	12	1a	728	27	954	954	27	High Ti
10044	12	1c	1220	30	781	781	23	High Ti
10044	644	2	877	26	536	536	57	High Ti
10044	644	8	421	22	—	—	—	High Ti
10044	644	4a	826	25	606	605	33	High Ti
10044	644	4b	1155	29	702	702	28	High Ti
75055	55	1	604	23	621	621	35	High Ti
75055	55	2	1225	35	794	794	26	High Ti
75055	55	3	1241	30	968	967	27	High Ti
75055	55	4	1430	34	794	794	26	High Ti
12039	42	4	1996	43	720	-	30	Low Ti
12039	42	6	2379	47	830	-	31	Low Ti
12039	42	17a	2784	95	729	-	28	Low Ti
12039	42	17b	2916	57	698	-	28	Low Ti
12040	211	1	105	21	9	-20	200 [†]	Low Ti
<i>12040</i>	<i>211</i>	<i>4</i>	<i>3</i>	<i>20</i>	<i>14</i>	<i>-900</i>	<i>150[†]</i>	<i>Low Ti</i>
<i>12040</i>	<i>211</i>	<i>5</i>	<i>16</i>	<i>20</i>	<i>-150</i>	<i>-340</i>	<i>35[†]</i>	<i>Low Ti</i>

* Background/blank subtracted. Detection limit (2σ) is ~20 ppm H₂O.

Italicized analyses have H₂O below detection limit, and are listed only for completeness.

‡ Corrected for spallation. See Deposit Material.

† Includes uncertainty on cosmic ray exposure age and spallogenic production rates; see text and Deposit Materials.

Figures

Figure 1. All (peer-reviewed) published δD and H_2O abundance data for apatites in mare basalts, including new data here (Table 1). Other data from (Greenwood et al., 2011; Barnes et al., 2013; Tartèse and Anand, 2013; Pernet-Fisher et al., 2014; Tartèse et al., 2014a; Tartèse et al., 2014b). Uncertainty bars are 2σ of counting statistics, and include uncertainties in spallation corrections. The majority of the analyses (at $\delta D > 200\%$) are consistent with a trend from high H_2O and lower δD values to low H_2O and high δD , consistent with H_2 degassing, see Figs. 2 and 3 of Tartèse and Anand (2013). A second group of analyses, with low H_2O and δD between $+200\%$ and -500% , includes many samples rich in the lunar KREEP component (especially the basalt 72275); see (Tartèse et al., 2014b).

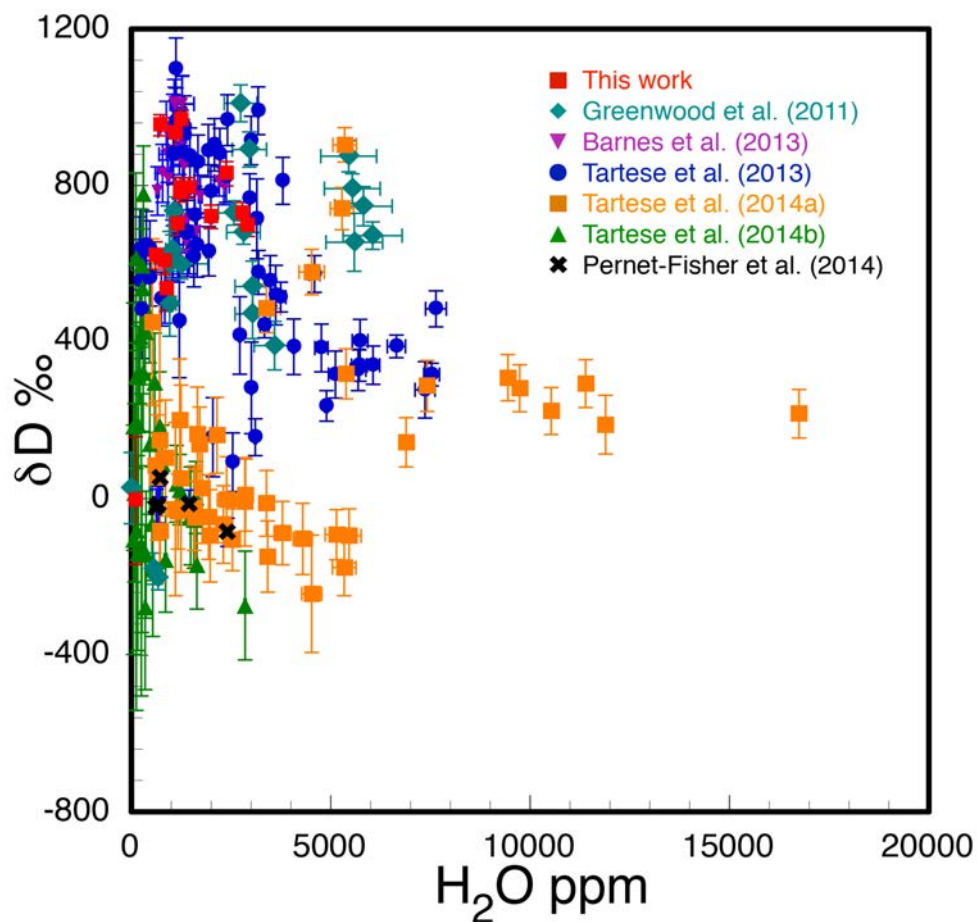
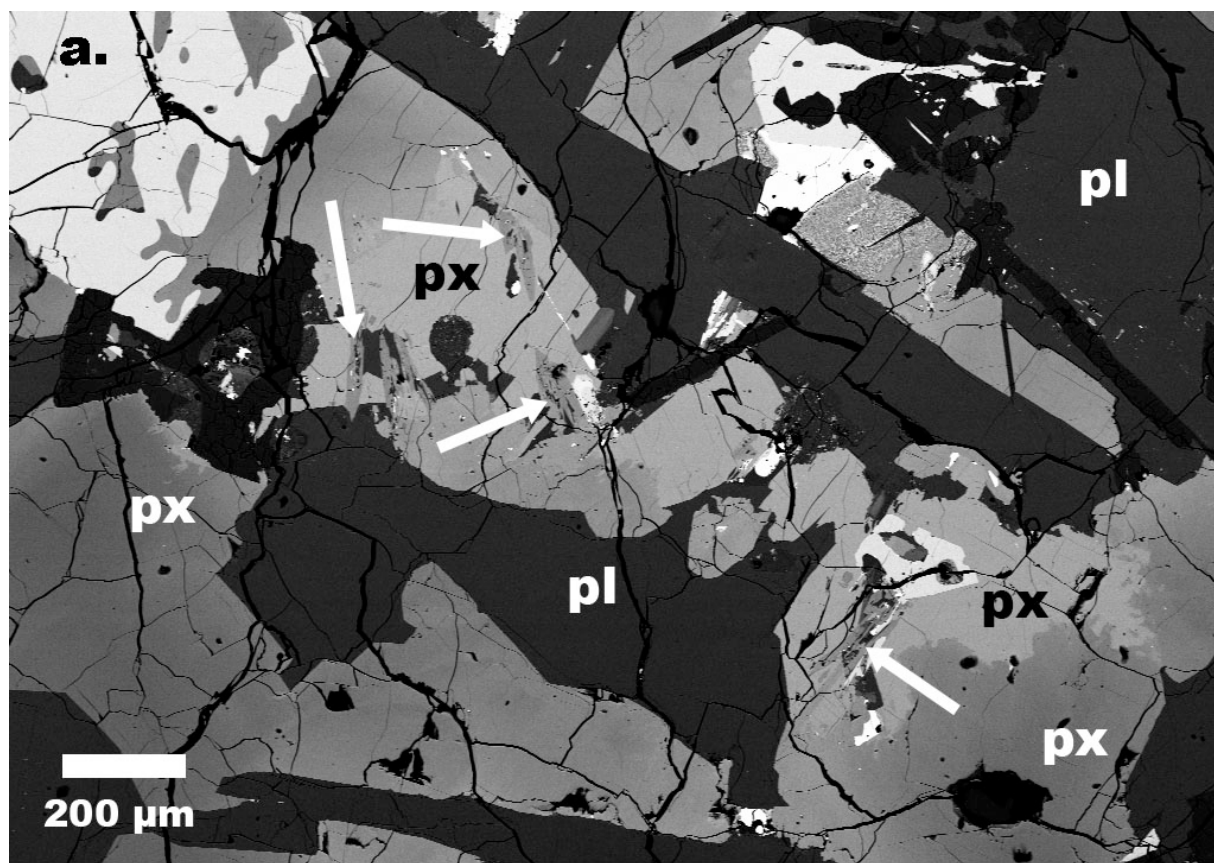


Figure 2. Backscattered electron images (BSE) of thin sections of apatite grains in lunar mare basalts; brightness is an approximate measure of mineral density, i.e. Mg# of pyroxene and olivine. Arrows denote apatite grains, px = pyroxene, pl = plagioclase, ol = olivine. [a] Basalt 75055, note brightness variations in its pyroxenes, which reflect variations in Mg#, showing that this basalt is chemically unequibrated. [b] Basalt 12040; note that pyroxene and olivine have relatively constant brightness (constant Mg#), indicating that this basalt is chemically equilibrated.



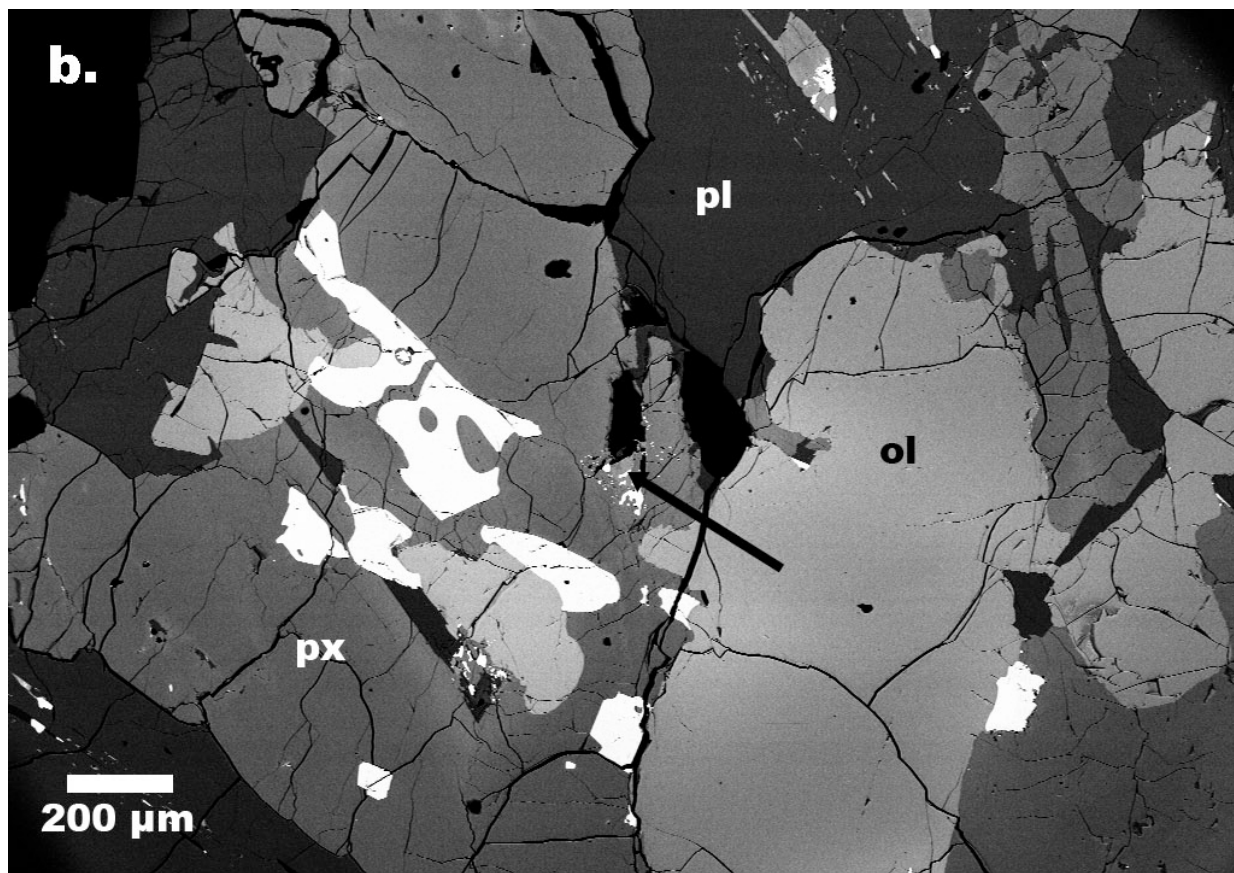


Figure 3. δD in apatites from lunar mare basalts versus $Mg\#_{\max} / Mg\#_{\min}$ in their pyroxenes, which is a measure of Fe-Mg heterogeneity, and thus a measure of their thermal and chemical equilibration histories. δD here is strongly correlated with $Mg\#_{\max} / Mg\#_{\min}$, which is interpreted as representing incorporation or exchange of regolith hydrogen, at $\delta D \leq -100\%$, into basalts that originally had high δD . Plotted δD values are averages by sample and data sources from Table S2; excluding only a few averages where other workers gave more precise data. Labeled data points referred to specifically in text; their data from: 14053 (Greenwood et al., 2011; Pernet-Fisher et al., 2014), Kalahari 009 (Tartèse et al., 2014b), 72275 (Tartèse et al., 2014a), NWA 4472 KREEP (Tartèse et al., 2014b), NWA 773 gabbro (Tartèse et al., 2014a), 12018 (Greenwood et al., 2014), and 12040 (this study; only grain 1, Table 1). Uncertainty bars for δD are 2σ of the distributions or of single analyses, whichever are larger (including uncertainty in cosmic ray exposure ages, and production rates of spallogenic D and H, as discussed in the text). Uncertainties on $Mg\#_{\max} / Mg\#_{\min}$ are not given, as these values from the literature are of uneven and unknown quality. Classifications are mostly from (Meyer, 2012).

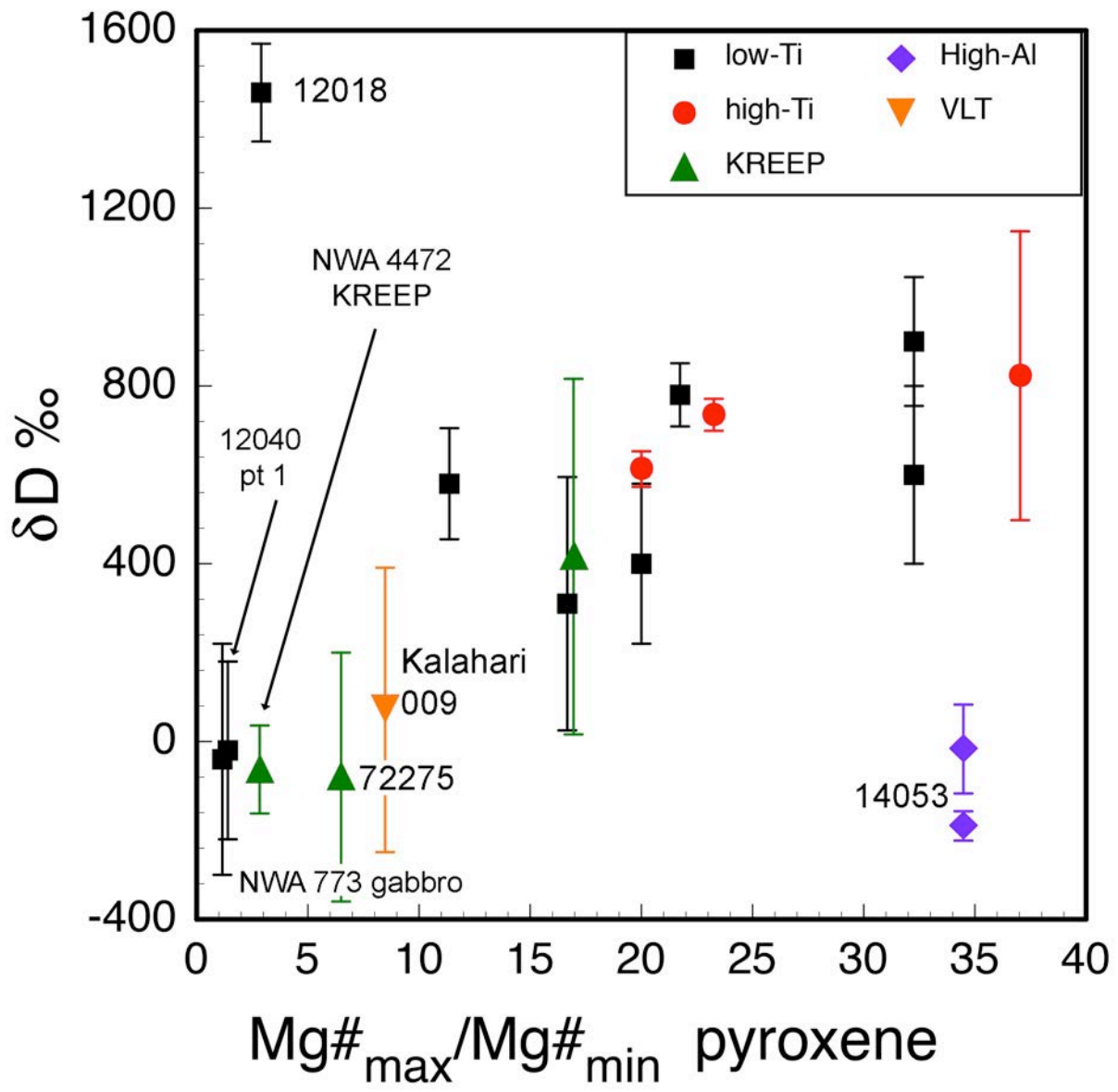
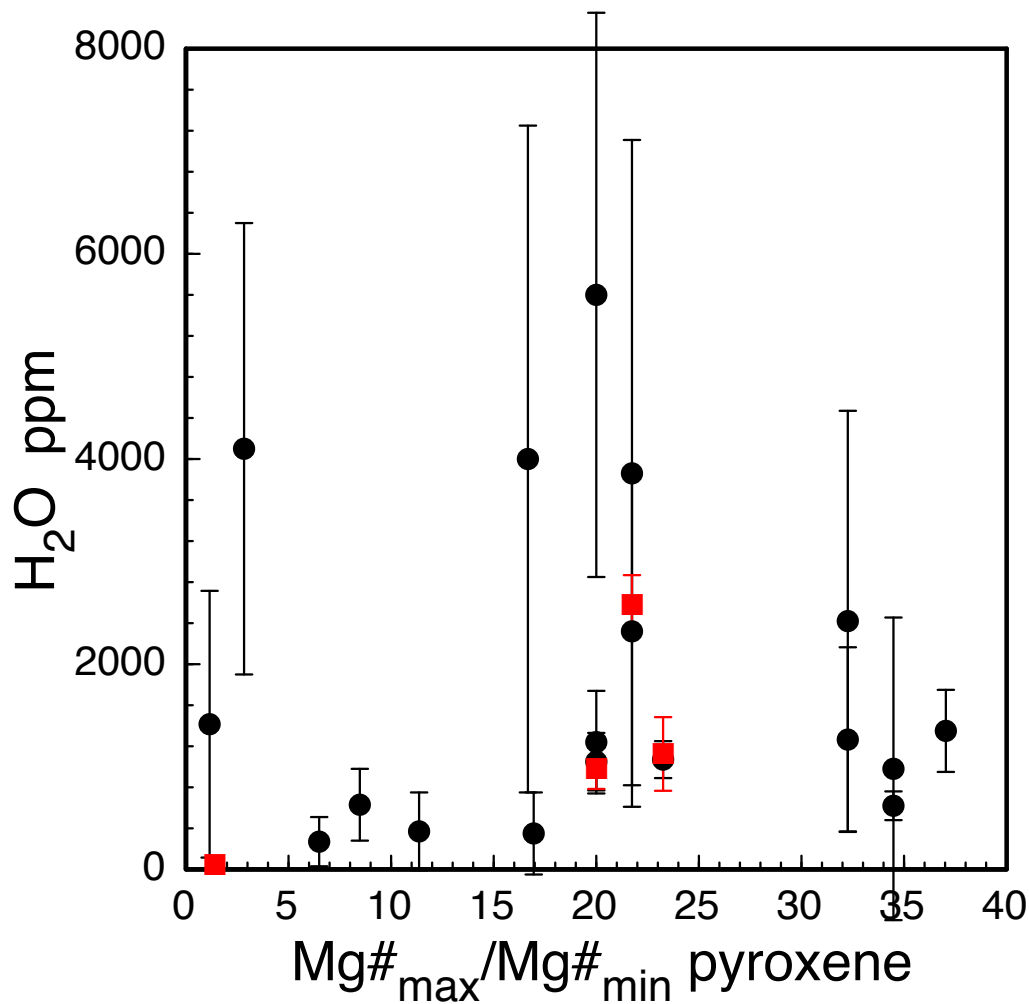


Figure 4. H₂O contents of mare basalt apatites, versus Mg_{#max}/Mg_{#min} in their pyroxenes, which is a measure of Fe-Mg heterogeneity, and thus a measure of their thermal and chemical equilibration histories (see Fig. 3).

Points are averages and 2σ for individual mare basalts as analyzed in different papers (see Table S2), the same selection as in Figure 3. Apatite H₂O contents show no correlation with pyroxene Mg_{#max}/Mg_{#min}. Red symbols are data obtained here; black points are from the literature (Table S2).



REFERENCES

- Alexander, C.M.O.D., Bowden, R., Fogel, M.L., Howard, K.T., Herd, C.D.K., and Nittler, L.R. (2012) The provenances of asteroids, and their contributions to the volatile inventories of the terrestrial planets. *Science*, 337, 721-723.
- Altwegg, K., Balsiger, H., Bar-Nun, A., Berthelier, J.-J., Bieler, A., Bochslers, P., Briouis, C., Calmonte, U., Combi, M., and De Keyser, J. (2015) 67P/Churyumov-Gerasimenko, a Jupiter family comet with a high D/H ratio. *Science*, 347(6220), 1261952.
- Anand, M., Tartèse, R., and Barnes, J.D. (2014) Understanding the origin and evolution of water in the Moon through lunar sample studies. *Philosophical Transactions of the Royal Society: A*, 372, 20130254.
- Barnes, J.J., Franchi, I.A., Anand, M., Tartèse, R., Starkey, N.A., Koike, M., and Russell, S.S. (2013) Accurate and precise measurements of the D/H ratio and hydroxyl content in lunar apatites using NanoSIMS. *Chemical Geology*, 337-338, 48-55.
- Barnes, J.J., Tartèse, R., Anand, M., McCubbin, F.M., Franchi, I.A., Starkey, N.A., and Russell, S.S. (2014) The origin of water in the primitive Moon as revealed by lunar highlands samples. *Earth and Planetary Science Letters*, 390, 244-252.
- Boctor, N.Z., Alexander, C.M.O.D., Wang, J., and Hauri, E.H. (2003) The sources of water in martian meteorites: Clues from hydrogen isotopes. *Geochimica Cosmochimica Acta*, 67(20), 3971-3989.
- Boyce, J.W., Eiler, J.M., and Channon, M.C. (2012) An inversion-based self-calibration for SIMS measurements: Application to H, F, and Cl in apatite. *American Mineralogist*, 97, 1116-1128.
- Boyce, J.W., and Hervig, R.L. (2008) Magmatic degassing histories from apatite volatile stratigraphy. *Geology*, 36(1), 63-66.
- (2009) Apatite as a monitor of late-stage magmatic processes at Volcán Irazú, Costa Rica. *Contributions to Mineralogy and Petrology*, 157, 135-145.
- Boyce, J.W., Liu, Y., Rossman, G.R., Guan, Y., Eiler, J.M., Stolper, E.M., and Taylor, L.A. (2010) Lunar apatite with terrestrial volatile abundances. *Nature*, 466, 466-469.
- Boyce, J.W., Tomlinson, S.M., McCubbin, F.M., Greenwood, J.P., and Treiman, A.H. (2014) The lunar apatite paradox. *Science*, 344, 400-402.
- Boyce, J.W., Treiman, A.H., Guan, Y., Ma, C., Eiler, J.M., Gross, J., Greenwood, J.P., and Stolper, E.M. (2015) The chlorine isotopic fingerprint of the lunar magma ocean. *Science Advances*, 1, e1500380.
- Burnett, D., Drozd, R., Morgan, C., and Podosek, F. (1975) Exposure histories of Bench Crater rocks. *Lunar and Planetary Science Conference Proceedings*, 6, p. 2219-2240.
- Chen, Y., Zhang, Y., Liu, Y., Guan, Y., Eiler, J., and Stolper, E.M. (2015) Water, fluorine, and sulfur concentrations in the lunar mantle. *Earth and Planetary Science Letters*, 427, 37-46.
- Cherniak, D.J., and Dimanov, A. (2010) Diffusion in pyroxene, mica, and amphibole. *Reviews in Mineralogy and Geochemistry*, 72, 641-690.
- Dyar, M.D., Hibbits, C.A., and Orlando, T.M. (2010) Mechanisms for incorporation of hydrogen in and on terrestrial planetary surfaces. *Icarus*, 298(1), 425-437.
- Elkins-Tanton, L.T., and Grove, T.L. (2011) Water (hydrogen) in the lunar mantle: Results from petrology and magma ocean modeling. *Earth and Planetary Science Letters*, 307, 173-179.
- Epstein, S., and Taylor, H.P. (1973) The isotopic composition and concentration of water, hydrogen, and carbon in some Apollo 15 and 16 soils and in the Apollo 17 orange soil. *4th Lunar Science Conference*, 2, 1559-1575.
- Fagan, A., Neal, C., Simonetti, A., Donohue, P., and O'Sullivan, K. (2013) Distinguishing between Apollo 14 impact melt and pristine mare basalt samples by geochemical and textural analyses of olivine. *Geochimica et Cosmochimica Acta*, 106, 429-445.

- Fagan, T., Taylor, G., Keil, K., Hicks, T., Killgore, M., Bunch, T., Wittke, J., Mittlefehldt, D., Clayton, R., and Mayeda, T. (2003) Northwest Africa 773: Lunar origin and iron-enrichment trend. *Meteoritics & Planetary Science*, 38(4), 529-554.
- Fagents, S.A., Rumpf, M.E., Crawford, I.A., and Joy, K.A. (2010) Preservation potential of implanted solar wind volatiles in lunar paleoregolith deposits buried by lava flows. *Icarus*, 207, 595-604.
- Fernandes, V.A., Burgess, R., and Turner, G. (2003) ^{40}Ar - ^{39}Ar chronology of lunar meteorites Northwest Africa 032 and 773. *Meteoritics and Planetary Science*, 38, 555-564.
- Friedman, I., Gleason, J.D., and Hardcastle, K.G. (1970) Water, hydrogen, deuterium, carbon, and C^{13} content of selected lunar material. *Proceedings of the Apollo 11 Lunar Science Conference*, 2, 1103-1109.
- Friedman, I., Hardcastle, K.G., and Gleason, J.D. (1974) Water and carbon in rusty lunar rock 66095. *Science*, 185(4148), 346-349.
- Füri, E., Deloule, E., Gurenko, A., and Marty, B. (2014) New evidence for chondritic lunar water from combined D/H and noble gas analyses of single Apollo 17 volcanic glasses. *Icarus*, 229, 109-120.
- Gibson, E.K., and Moore, G.W. (1973) Volatile-rich lunar soil: evidence of possible cometary impact. *Science*, 179(4068), 69-71.
- Greenwood, J.P., Itoh, S., Sakamoto, N., Warren, P.H., A, T.L., and Yurimoto, H. (2011) Hydrogen isotope ratios in lunar rocks indicate delivery of cometary water to the Moon. *Nature Geoscience*, 4, 79-82.
- Greenwood, J.P., Itoh, S., Sakamoto, N., Yanai, K., Singer, J.A., and Yurimoto, H. (2014) Hydrogen isotopes of water in the Moon: Evidence for the giant impact model from melt inclusions and apatite in Apollo rock samples. *Lunar and Planetary Science Conference*, 45, p. Abstract #2707.
- Hartogh, P., Lis, D.C., Bockelée-Morvan, D., de Val-Borro, M., Biver, N., Küppers, M., Emprechtinger, M., Bergin, E.A., Crovisier, J., and Rengel, M. (2011) Ocean-like water in the Jupiter-family comet 103P/Hartley 2. *Nature*, 478(7368), 218-220.
- Hauri, E.H., Saal, A.E., Rutherford, M.C., and Van Orman, J.A. (2015) Water in the Moon's interior: Truth and consequences. *Earth and Planetary Science Letters*, 409, 252-264.
- Hauri, E.H., Wienreich, T., Saal, A.E., Rutherford, M.C., and Van Orman, J.A. (2011) High pre-eruptive water contents preserved in lunar melt inclusions. *Science*, 333, 213-215.
- Hui, H., Guan, Y., Chen, Y., Peslier, A.H., Zhang, Y., Liu, Y., Rossman, G.R., Eiler, J.M., and Neal, C.R. (2015) SIMS analysis of water abundance and hydrogen isotope in lunar highland plagioclase. *Lunar and Planetary Science Conference*, 46, Abstract #1927.
- Hui, H., Pelsier, A.H., Zhang, H., and Neal, C.R. (2013) Water in lunar anorthosites and evidence for a wet early Moon. *Nature Geoscience*, 6, 177-180.
- Jolliff, B.L., Korotev, R.L., Zeigler, R.A., and Floss, C. (2003) Northwest Africa 773: Lunar mare breccia with a shallow-formed olivine-cumulate component, inferred very-low-Ti (VLT) heritage, and a KREEP connection. *Geochimica et Cosmochimica Acta*, 67(24), 4857-4879.
- Joy, K.H., Burgess, R., Hinton, R., Fernandes, V., Crawford, I.A., Kearsley, A., and Irving, A. (2011) Petrogenesis and chronology of lunar meteorite Northwest Africa 4472: A KREEPy regolith breccia from the Moon. *Geochimica et Cosmochimica Acta*, 75(9), 2420-2452.
- Liu, Y., Guan, Y., Zhang, Y., Rossman, G.R., Eiler, J.M., and Taylor, L.A. (2012a) Direct measurement of hydroxyl in the lunar regolith and the origin of lunar surface water. *Nature Geoscience*, 5, 779-782.
- Liu, Y., Mosenfelder, J., Guan, Y., Rossman, G., Eiler, J., and Taylor, L. (2012b) SIMS analysis of water abundance in nominally anhydrous minerals in lunar basalts. *Lunar and Planetary Science Conference*, 43, Abstract #1866.
- Lorenzetti, S., Busemann, H., and Eugster, O. (2005) Regolith history of lunar meteorites. *Meteoritics and Planetary Science*, 40, 315-327.

- McCubbin, F.M., Steele, A., Hauri, E.H., Nekvasil, H., Yamashita, S., and Hemley, R.J. (2010) Nominally hydrous magmatism on the Moon. *Proceedings of the National Academy of Sciences*, 107, 11223-11228.
- McCubbin, F.M., Vander Kaaden, K.E., Tartèse, R., Klima, R.L., Liu, Y., Mortimer, J., Barnes, J.J., Shearer, C.K., Treiman, A.H., and Lawrence, D.J. (2015) Magmatic volatiles (H, C, N, F, S, Cl) in the lunar mantle, crust, and regolith: Abundances, distributions, processes, and reservoirs. *American Mineralogist*, 100, 1668-1707.
- Merlivat, L., Lelu, M., Nief, G., and Roth, E. (1976) Spallation deuterium in rock 70215. *Proceedings of the Lunar and Planetary Science Conference*, 7th, 649-658.
- Meyer, C. (2012) *Lunar Sample Compendium*. NASA.
- O'Reilly, S.Y., and Griffin, W.L. (2000) Apatite in the mantle: implications for metasomatic processes and high heat production in Phanerozoic mantle. *Lithos*, 53, 217-232.
- Patiño Douce, A.E., and Roden, M. (2006) Apatite as a probe of halogen and water fugacities in the terrestrial planets. *Geochimica Cosmochimica Acta*, 70, 3173-3196.
- Pernet-Fisher, J., Howarth, G., Liu, Y., Chen, Y., and Taylor, L. (2014) Estimating the lunar mantle water budget from phosphates: Complications associated with silicate-liquid-immiscibility. *Geochimica et Cosmochimica Acta*, 144, 326-341.
- Pieters, C.M., Goswami, J.N., Clark, R.N., Annadurai, M., Boardman, J., Buratti, B., Combe, J.-P., Dyar, M.D., Green, R., Head, J.W., Hibbits, C., Hicks, M., Isaacson, P., Klima, R., Kramer, G., Kumar, S., Livo, E., Lundeen, S., Malaret, E., McCord, T., Mustard, J., Nettles, J., Petro, N.E., Runyon, C., Staid, M., Sunshine, J., Taylor, L.A., Tompkins, S., and Varanasi, P. (2009) Character and spatial distribution of OH/H₂O on the surface of the Moon seen by M³ on Chandrayaan-1. *Science*, 326(5952), 568-572.
- Reedy, R.C. (1981) Cosmic-ray-produced stable nuclides: Various production rates and their implications. *Proceedings of Lunar and Planetary Science*, 12, 1809-1823.
- Robinson, K.L., and Taylor, G.J. (2014) Heterogeneous distribution of water in the Moon. *Nature Geoscience*, 7(6), 401-408.
- Rumpf, M.E., Fagents, S.A., Crawford, I.A., and Joy, K.A. (2013) Numerical modeling of lava-regolith heat transfer on the Moon and implications for the preservation of implanted volatiles. *Journal of Geophysical Research: Planets*, 118, 382-397.
- Saal, A.E., Hauri, E.H., Lo Cascio, M., Van Orman, J.A., Rutherford, M.C., and Cooper, R.F. (2008) Volatile content of lunar volcanic glasses and the presence of water in the Moon's interior. *Nature*, 454, 192-195.
- Saal, A.E., Hauri, E.H., Van Orman, J.A., and Rutherford, M.C. (2013) Hydrogen isotopes in lunar volcanic glasses and melt inclusions reveal a carbonaceous chondrite heritage. *Science*, 340, 1317-1320.
- Stephant, A., and Robert, F. (2014) The negligible chondritic contribution in the lunar soils water. *Proceedings of the National Academy of Sciences*, 111(42), 15007-15012.
- Tartèse, R., and Anand, M. (2013) Late delivery of chondritic hydrogen into the lunar mantle: Insights from mare basalts. *Earth and Planetary Science Letters*, 361, 480-486.
- Tartèse, R., Anand, M., Barnes, J.J., Starkey, N.A., Franchi, I.A., and Sano, Y. (2013) The abundance, distribution, and isotopic composition of hydrogen in the Moon as revealed by basaltic lunar samples: Implications for the volatile inventory of the Moon. *Geochimica Cosmochimica Acta*, 122, 58-74.
- Tartèse, R., Anand, M., Joy, K.H., and Franchi, I.A. (2014a) H and Cl isotope systematics of apatite in brecciated lunar meteorites Northwest Africa 4472, Northwest Africa 773, Sayh al Uhaymir 169, and Kalahari 009. *Meteoritics & Planetary Science*, 49(12), 2266-2289.
- Tartèse, R., Anand, M., McCubbin, F.M., Elardo, S.M., Shearer Jr, C.K., and Franchi, I.A. (2014b) Apatites in lunar KREEP basalts: The missing link to understanding the H isotope systematics of the Moon. *Geology*, 42, 363-366.

- Taylor, L.A., Patchen, A., Mayne, R.G., and Taylor, D.H. (2004) The most reduced rock from the moon, Apollo 14 basalt 14053: its unique features and their origin. *American Mineralogist*, 89, 1617-1624.
- Treiman, A.H. (2005) The nakhlite Martian meteorites: Augite-rich igneous rock from Mars. *Chemie der Erde*, 65, 203-270.
- Treiman, A.H., Boyce, J.W., Gross, J., Guan, Y., Eiler, J.M., and Stolper, E.M. (2014) Phosphate-halogen metasomatism of lunar granulite 79215: Impact-induced fractionation of volatiles and incompatible elements. *American Mineralogist*, 99(10), 1860-1870.
- Ustunisik, G., Nekvasil, H., Lindsley, D.H., and McCubbin, F.M. (2015) Degassing pathways of Cl-, F-, H-, and S-bearing magmas near the lunar surface: Implications for the composition and Cl isotopic values of lunar apatite. *American Mineralogist*, 100(8-9), 1717-1727.
- Watson, L.L., Hutcheon, I.D., Epstein, S., and Stolper, E. (1994) Water on Mars: Clues from deuterium/hydrogen and water contents of hydrous phases in SNC meteorites. *Science*, 265(5168), 86-90.
- Zeigler, R., Korotev, R., and Jolliff, B. (2007) Petrography, geochemistry, and pairing relationships of basaltic lunar meteorite stones NWA 773, NWA 2700, NWA 2727, NWA 2977, and NWA 3160. *Lunar and Planetary Science Conference*, 38, p. Abstract #2109.